

# Optical characterization of an unknown single layer: Institut Fresnel contribution to the Optical Interference Coatings 2004 Topical Meeting Measurement Problem

Fabien Lemarchand, Carole Deumié, Myriam Zerrad, Laëtitia Abel-Tiberini, Bertrand Bertussi, Gaëlle Georges, Basile Lazaridès, Michel Cathelinaud, Michel Lequime, and Claude Amra

We present the characterizations performed at the Institut Fresnel for the Measurement Problem of the Optical Interference Coatings 2004 Topical Meeting. A single layer coated on a fused-silica substrate of unknown composition and parameters is analyzed in terms of optogeometrical parameters, uniformity, and scattering. We determine the refractive index and the average thickness of the coating, then provide the localized determination of the thickness with a 2 mm spatial resolution. Topography measurements include atomic force microscopy and angle-resolved scattering measurements. These results are completed thanks to a Taylor Hobson noncontact 3D surface profiler. © 2006 Optical Society of America  
*OCIS codes:* 310.0310, 240.0310, 310.6860, 310.6870, 310.1620.

## 1. Introduction

The Optical Interference Coatings Topical Meeting (OIC) introduced a measurement problem for the first time in 2004. It was organized by Angela Duparré from the Fraunhofer Institut Angewandte Optik und Feinmechanik (IOF) and Detlev Ristau from Laser Zentrum Hannover e.V. Participants were asked to investigate three tasks—optical parameters, roughness, and additional measurements—on an unknown single layer coated on a fused-silica substrate (Suprasil2 from Heraeus) that was 25 mm in diameter and 1 mm thick. The different samples, placed on the same equal radial position, were coated at IOF Jena. Of course, participants were only informed of the nature of the layer ( $\text{HfO}_2$  coated with Advanced Plasma Source technology) during the meeting session. In this paper, we present the different characterization results obtained by Institut Fresnel on the sample numbered OIC3 and sent to the Measurement Problem organizers before the meeting.

## 2. Spectrophotometric Measurements

### A. Measurement Procedure

The measurements of reflectance and transmittance in the UV–visible range are first performed with a dual-beam commercial spectrophotometer (Lambda 18, Perkin-Elmer) with a V-W accessory. The beam aperture is about 5 mm  $\times$  7 mm with an incidence of 7.5° on the sample. Transmitted and reflected fluxes on each side of the OIC3 sample are compared with those of our reference substrate, UV fused silica that is 1 mm thick and whose characteristics are similar to those of Corning 7980. The reflectance and transmittance of a semi-infinite substrate (without a substrate backside) are then calculated thanks to the data of the refractive index of the OIC sample substrate (Suprasil2). The wavelength resolution is fixed at 1 nm, and measurements are performed from 200 to 900 nm. Note that, above 860 nm, the sensitivity of the detector is weak, inducing noisy data. The spectral interval between two data points is fixed at 2 nm (351 data points from 200 to 900 nm). The precision of the measurement data is better than 0.1% (absolute value) for transmission and 0.5% for reflection from 200 to 850 nm. Unfortunately, a comparison with a Suprasil2 bare substrate identical to those of OIC3 was not possible. Indeed, we use a comparative method to extract the reflectance and transmittance data. The analyses of the transmitted and reflected

---

The authors are with the Institut Fresnel UMR CNRS 6133, Université Paul Cézanne, Domaine Universitaire de Saint-Jérôme, 13397 Marseille Cedex 20, France. F. Lemarchand's e-mail address is fabien.lemarchand@fresnel.fr.

Received 28 February 2005; accepted 14 July 2005.

0003-6935/06/071312-07\$15.00/0

© 2006 Optical Society of America

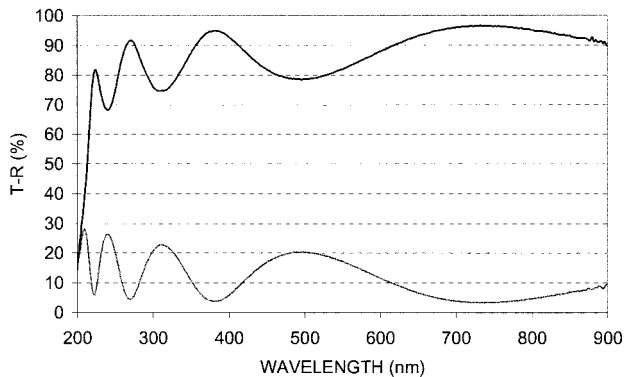


Fig. 1. Reflectance (gray curve) and transmittance (black curve) as a function of wavelength corresponding to a semi-infinite substrate (without backside reflectance).

flux ratio leads to the major hypothesis that the intrinsic properties of both substrates (bare and UV silica) and the coated sample (Suprasil2) are perfectly identical. Because of their different nature, the errors between the true and the theoretical (i.e., as given by the manufacturer) properties are not compensated. This is especially verified in the near-UV range. The measured reflectance and transmittance (semi-infinite substrate) as a function of wavelength are given in Fig. 1. Losses are below 1% for wavelengths above 400 nm.

#### B. Determination of Optogeometrical Parameters

The determination of the optogeometrical parameters of the layer is performed with three different methods.  $n(\lambda)$  and  $k(\lambda)$  are the real and imaginary parts of the refractive index, respectively, and  $d$  is the thickness of the layer.

The first method, M1, uses commercial software, Optichar from Optilayer (<http://www.optilayer.com>). For  $n(\lambda)$  the selected method uses a Cauchy formula then a refinement with arbitrary dispersion, and for  $k(\lambda)$  a UV-visible formula then a refinement with arbitrary dispersion. A satisfying fitting agreement is

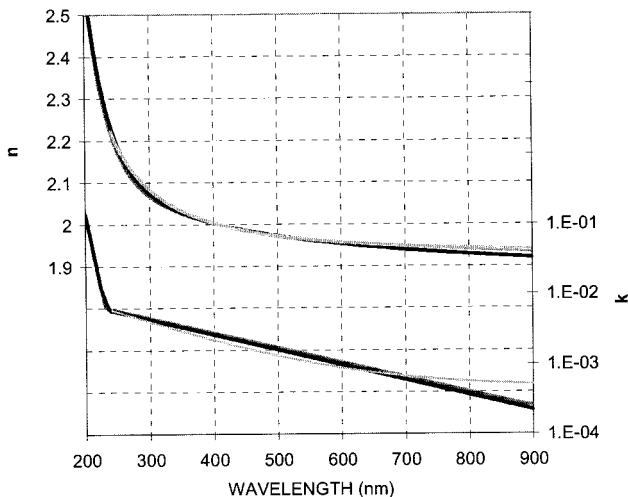


Fig. 2. Refractive index determination by M1 (light gray curves), M2 (gray curves), and M3 (black curves).

Table 1. Comparison between Three Index Determination Methods

	Determination Method		
	M1	M2	M3
Number of data points	331	351	351
Lambda min	240 nm	200 nm	200 nm
Lambda max	900 nm	900 nm	900 nm
Discrepancy ( $D$ )	0.20%	0.40%	0.28%
Thickness ( $d$ )	189.4 nm	190.4 nm	189.7 nm
$n$ (240 nm)	2.223	2.218	2.235
$k$ (240 nm)	0.0059	0.0061	0.0058
$n$ (400 nm)	2.003	2.003	2.003
$k$ (400 nm)	0.0022	0.0028	0.0026
$n$ (600 nm)	1.956	1.954	1.953
$k$ (600 nm)	0.009	0.0011	0.001
$n$ (800 nm)	1.942	1.941	1.928
$k$ (800 nm)	0.0006	0.0004	0.0004

observed when removing measurements below 240 nm. This reduced range of wavelengths can be explained by the difficulty of correctly determining  $k(\lambda)$  with prerecorded formulas. Even when an arbitrary profile index for  $k(\lambda)$  is used, the agreement between fitted and experimental data remains relatively poor in the whole 200–900 nm range. Refinements concerning possible inhomogeneities yield insignificant improvement of the fit.

The second method, M2, developed at the Institut Fresnel some years ago,<sup>1</sup> consists of first determining the values of the refractive index  $n$  for wavelengths corresponding to extrema of the reflectance curve. A Cauchy formula is assumed for wavelengths between reflectance extrema, and the value of the film thickness  $d$  is determined. This solution is the starting solution for the refractive index values. Then iterative calculations using the simplex method enable us to determine the values of  $n$  and  $k$  that fit the optical measurements at each wavelength. The value of  $d$  is also iteratively optimized. Finally, curves of  $n(\lambda)$  and  $k(\lambda)$  are fitted to obtain regular behaviors. The inhomogeneities estimated by the program are once again insignificant.

The third method, M3, is based on the optimization

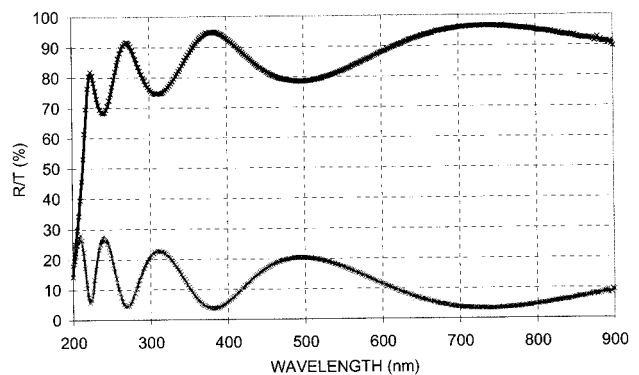


Fig. 3. Fit between experimental and theoretical (M3) reflectance (gray) and transmittance (black). Crosses, experimental values; curves, theoretical values.

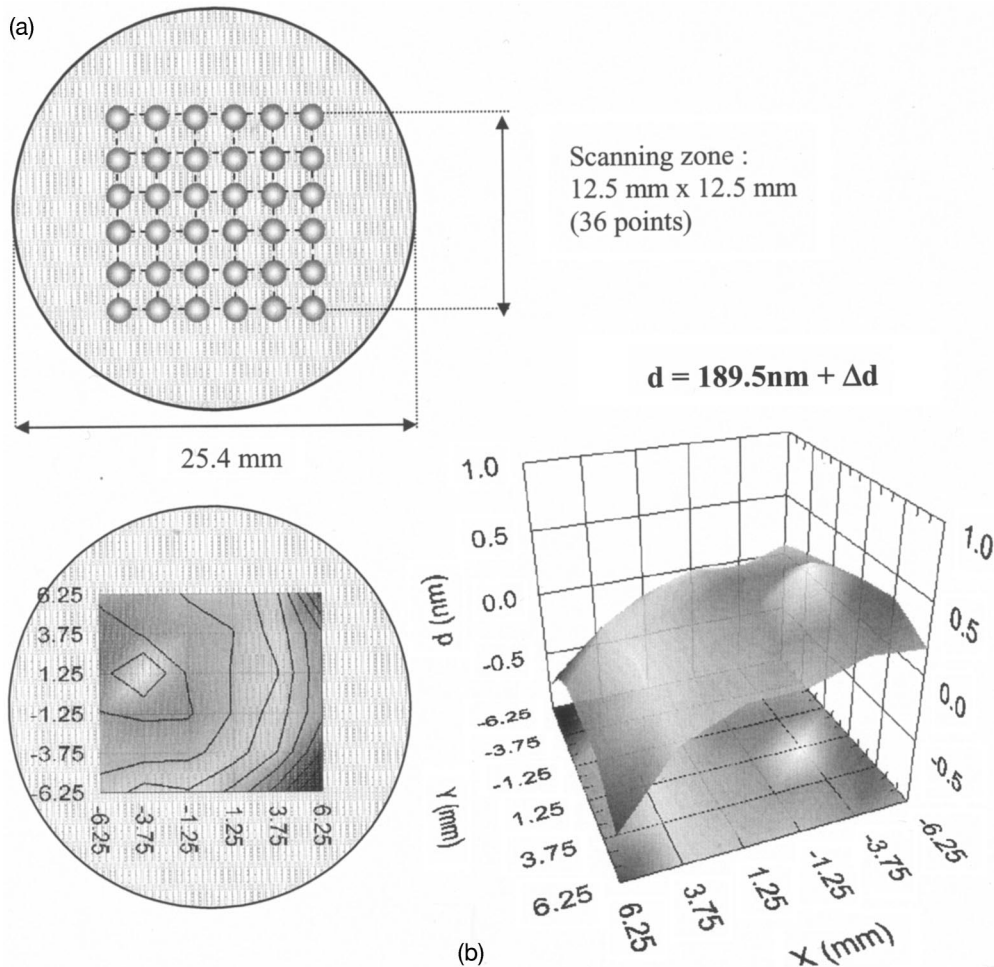


Fig. 4. Spatial distribution of the thickness of the coating.

of a set of parameters including the film thickness  $d$  and several parameters suitable for describing the refractive index and the extinction coefficient as a function of the wavelength given by

$$n(\lambda) = a_0 + a_2/\lambda^2 + a_3/\lambda^3 + a_4/\lambda^4 + a_5/\lambda^5,$$

$$k(\lambda) = b_1/\lambda^{b_2}. \quad (1)$$

A multidimensional interval is clustered into regions, and for each region a local minimum for  $(a_0, a_1, a_2, a_3, a_4, a_5, b_1, b_2)$  is seeded by use of a simplex algorithm. Then the interval is reduced around the best local minimum, and the process is iteratively repeated with a smaller region of attraction, as for simulated annealing methods. When the values of  $n$  and  $d$  are definitely fixed,  $k$  is optimized for each wavelength. Finally,  $k(\lambda)$  is fitted to obtain regular behaviors.

The corresponding refractive indices and thicknesses as functions of wavelength for the three described methods are plotted in Fig. 2, and some points of comparison are given in Table 1. The values of the refractive index are similar for the three methods, with dispersion for values of  $n$  being about 0.01 for each wavelength. The values of  $k$  are also similar for

the three methods, with dispersion values around 0.001. For wavelengths above 700 nm, measurements are not accurate enough to give a significant value of  $k$ . For  $\lambda$  above 700 nm,  $k$  is below 0.0007. The nominal thickness  $d$  is about 189.5 nm.

To compare the results given by the different methods, we can define a defect function  $D$  as

$$D = \frac{1}{2N_{\text{data}}} \sum_{i=1}^{N_{\text{data}}} \left[ \frac{T_{\text{exp}}(\lambda_i) - T_{\text{fitted}}(\lambda_i)}{100} \right]^2 + \left[ \frac{R_{\text{exp}}(\lambda_i) - R_{\text{fitted}}(\lambda_i)}{100} \right]^2, \quad (2)$$

where  $R$  and  $T$  correspond to the reflectance and transmittance, respectively, for a semi-infinite substrate and are normalized to 100%.  $D$  is the average rms error between fitted and measured data determined with the three methods described above. The most satisfying result is given by M3. In Fig. 3 we plot the agreement between the theoretical reflectance and transmittance given by M3 and measurements.

The uncertainties of  $n$ ,  $k$ , and  $d$  are mainly linked to the measurement method. As explained above, this comparative method is not reliable with substrates of different natures (geometrical and optical properties).

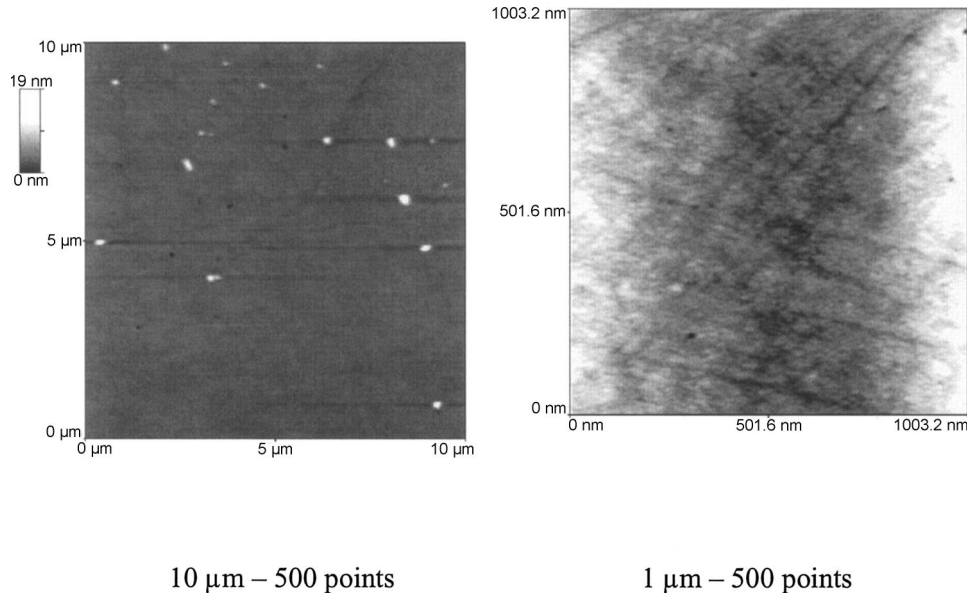


Fig. 5. AFM measurements of face 1.

Unfortunately, the comparison between a Suprasil2 bare substrate identical to those of OIC3 was not possible. Using our described method, we performed several sets of measurements and determined  $n$ ,  $k$ , and  $d$  with the three methods described. The standard deviations we obtained are  $\pm 0.01$  for values of  $n$ ,  $\pm 0.001$  for values of  $k$ , and  $\pm 1$  nm for values of  $d$ .

### C. Measurement of the Coating Uniformity

The principle of measurement of the uniformity of a coating is precisely described in Ref. 2. Here is a brief presentation of the procedure followed in the case of the OIC Measurement Problem: We perform a local measurement of the transmittance as a function of the wavelength under normal incidence thanks to a spectrum analyzer (Ando AQ 6315A). The incident beam is a disk of 2 mm diameter, and the flux transmitted through the OIC3 sample is recorded from 400 to 1350 nm for an area of  $6 \times 6$  points of the sample's surface. The distance between two adjacent points is 2.5 mm [see Fig. 4(a)]. The wavelength resolution of the spectrum analyzer is about 5 nm, and 1000 data points are recorded for each spectrum acquisition. The analysis zone is automatically scanned thanks to a double-axis  $X/Y$  motorization. For each point, the spectral measurements are compared to a reference channel to compensate the eventual fluctuations of the halogen light source.

Then the relative transmitted flux (with and without the OIC sample) is analyzed thanks to OptiChar software with the following procedure: First the refractive index with a Cauchy formula and the nominal thickness of the unknown layer are determined with a standard procedure for several points. Then an average Cauchy formula is definitely fixed for the layer. The local thickness is then calculated for each point. Note that this procedure is sensitive to the optical thickness and that we are not able to distinguish a local variation of  $n$  from a variation of  $d$ . As a

consequence, we are able to draw a mapping of the local thickness (optical thickness to be exact).

In Fig. 4(b) we plot the difference between the local and the nominal measured thicknesses of the OIC3 sample as a function of the incident beam position. The analysis of the 36 different thicknesses shows a maximal difference of thickness (amplitude) equal to 1.2 nm and a standard deviation (square root of the variance) of about 0.3 nm. The mean thickness is 189.5 nm. These values correspond to a maximal error of uniformity of 0.6%.

## 3. Topography Measurements

### A. Atomic Force Microscopy Measurement Procedure

Atomic force microscopy (AFM) measurements are performed with a commercial apparatus (Topometrix Thermomicroscope Explorer with a standard pyramidal tip). Experimental conditions are defined by the OIC Measurement Problem, that is, 10  $\mu\text{m}$  and 1  $\mu\text{m}$  sizes with  $500 \times 500$  data points. Results of the AFM measurements for the two scan lengths are depicted in Fig. 5 on the coated face of the sample (Face 1). These measurements reveal the presence of numerous pits on the surface. The density of defects is about 16 per 100  $\mu\text{m} \times 100 \mu\text{m}$  area. Some sections of one of these pits are given in Fig. 6. The rms roughness

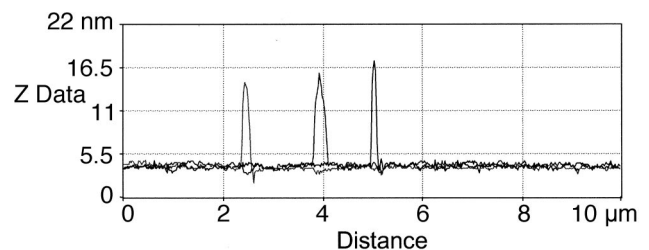
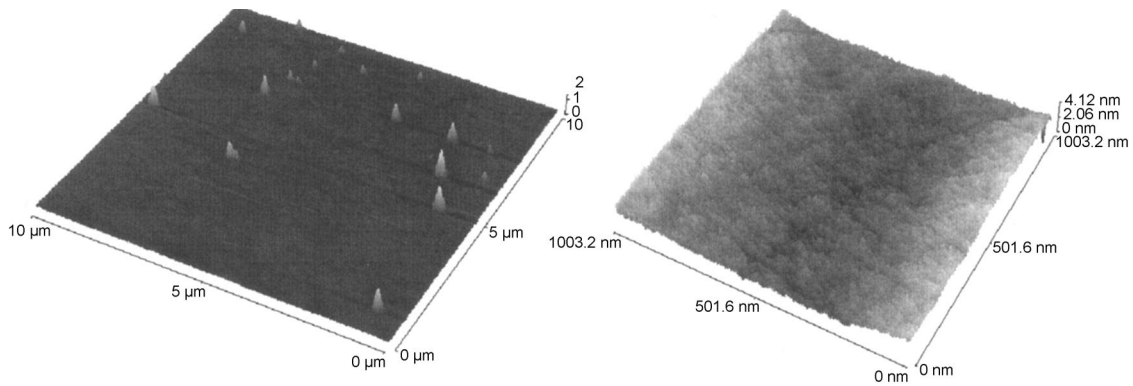


Fig. 6. Sections of some dust on the surface.



10 μm – 500 points

1 μm – 500 points

Fig. 7. AFM measurements of face 1: 3D views.

values for face 1 are 0.57 nm for the 10 μm image on the whole image, 0.27 nm for a 5 μm area without pits, and 0.24 nm for the 1 μm image (no pits). In the case of the 10 μm image, the rms value clearly corresponds to the presence of pits, whereas on the 1 μm image, it depends only on the intrinsic roughness of the sample. Moreover, the nonstationarity of the roughness may explain discrepancies.

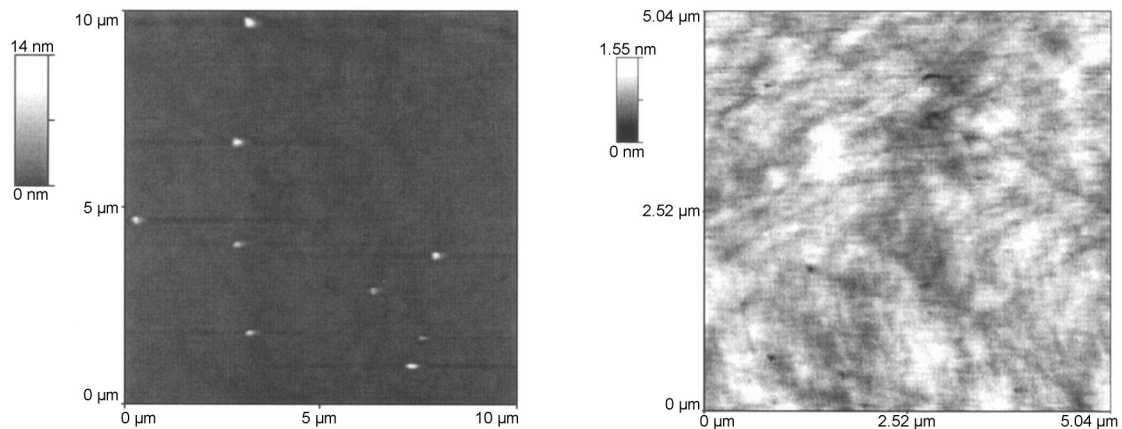
Three-dimensional views of the same measurements are given in Fig. 7. The pits are again present on the second face of the sample, as we can see in Fig. 8. The rms roughness values are as follows: for the 10 μm image, 0.47 and 0.29 nm on a 5 μm area without pits, and for the 5 μm image, 0.18 nm (no pits).

We can extract from these measurements the roughness spectra of the surfaces, defined by

$$\gamma(\sigma) = \frac{4\pi^2}{S} |\hat{h}(\sigma)|^2 = \left(\frac{2\pi}{L}\right)^2 |\hat{h}(\sigma)|^2. \quad (3)$$

This roughness spectrum is calculated in a frequency bandwidth<sup>3,4</sup> defined by the sampling interval  $B(L) = [2\pi/L, N\pi/L]$ , where  $L$  is the size of the measured area and  $N$  is the number of points per line. Notice here that we consider spatial pulsations equal to spatial frequency times  $2\pi$ . Moreover, the spectra are averaged over a polar angle.

We can notice on Fig. 9 that the roughness spectra do not perfectly overlap at the intersection of the two pulsation bandwidths reached by the two measurements with different sampling rates. This phenomenon is due to the presence of numerous pits on the surface and to nonstationarity. These pits are visible on the surface measured with a size of 10 μm, but not on the measurement with a size of 1 μm, which reveals only the intrinsic roughness. Under these conditions, the shape of the roughness spectrum corresponding to the 10 μm image reveals a bump connected with the presence of dust and cannot overlap with the spectrum of the 1 μm surface. We find



10 μm – 500 points

5 μm – 500 points

Fig. 8. AFM measurements of face 2.

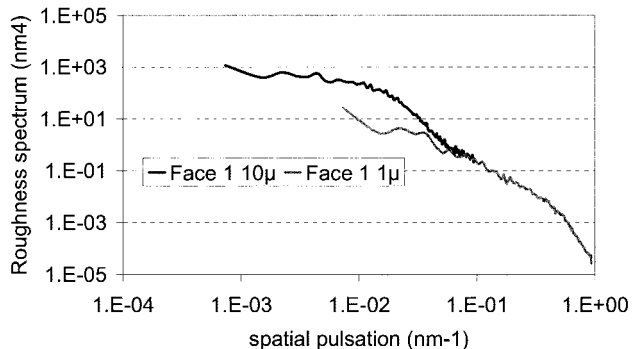


Fig. 9. Roughness spectra obtained from AFM measurements of face 1.

the same phenomenon on the second face of the sample (Fig. 10).

### B. Light-Scattering Measurements

Angle-resolved scattering (ARS) measurements<sup>5-9</sup> were performed on the same sample at a wavelength of 633 nm (see Fig. 11). Notice the presence of numerous pits on the surface of the sample, which are responsible for a great part of the light scattering. The roughness spectrum can be deduced from light-scattering measurements, thanks to specific theoretical investigations corresponding to the prediction of light scattering from multilayer components (first-order theory),<sup>6,7</sup> because the sample is composed of a single layer deposited on a silica substrate, as described in Section 1. For these calculations we used the characteristics of the materials deduced from Section 2 (at a wavelength of 633 nm,  $n = 1.457$  for the substrate,  $n = 1.93$  for the layer with a geometrical thickness about 190 nm). The rms roughness was then extracted thanks to the integration of the roughness spectrum on the frequency bandwidth. The rms roughness is about 1 nm (for a diameter of the light beam at the sample surface of about 2 mm at a wavelength of 633 nm).

### C. Comparison between Atomic Force Microscopy and Angle-Resolved Scattering Measurements

AFM and ARS measurements can be compared.<sup>3,5,10</sup> These two techniques permit us to deduce the rough-

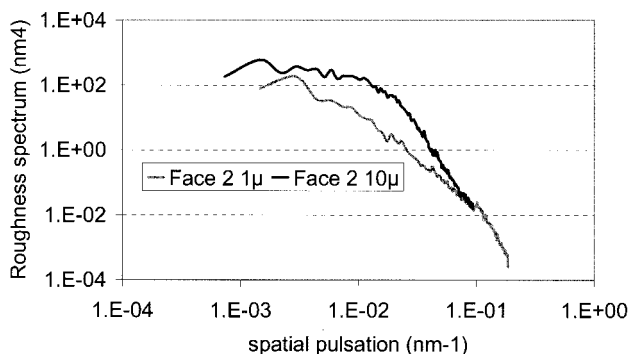


Fig. 10. Roughness spectra obtained from AFM measurements of face 2.

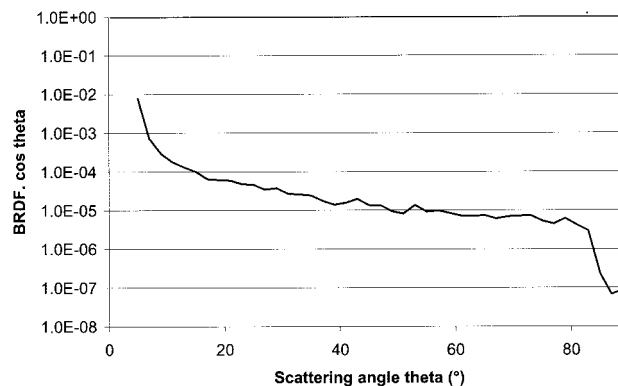


Fig. 11. Angular scattering measurements on the OIC sample. BRDF, bidirectional reflectance distribution function.

ness spectrum in different frequency bandwidths, depending on the sampling rate for AFM measurements and on the wavelength in the case of ARS measurements: In the case of AFM,  $B(L) = [2\pi/L, N\pi/L]$  as in Subsection 3.A; in the case of ARS,  $B(\lambda) = [2\pi \sin \theta_{\min}/\lambda, 2\pi/\lambda]$ , where  $\lambda$  is the emitted wavelength and  $\theta_{\min}$  is the minimum scattering angle determined by the mechanical conditions.

Both techniques can be applied to the same frequency domain provided that the ARS wavelength is twice the AFM sampling interval ( $N\pi/L = 2\pi/\lambda$ ). In the case of the OIC measurements, the AFM specifications (10  $\mu\text{m}$  for 500 points) should correspond to UV measurements.

ARS measurements are performed at a wavelength equal to 633 nm (see Fig. 11). The roughness spectrum and the rms roughness are deduced from ARS measurements as described before. The three spectra are shown in Fig. 12. The discrepancies may result from the presence of pits.

### D. Additional Measurements

Additional topographic measurements are achieved on the OIC3 sample with the help of a Taylor Hobson noncontact 3D surface profiler (Talysurf CCI 3000) equipped with a  $\times 20$  Mireau microscope objective. More than  $10^6$  data points are collected over areas of  $0.9 \text{ mm} \times 0.9 \text{ mm}$ . The surface profile is represented

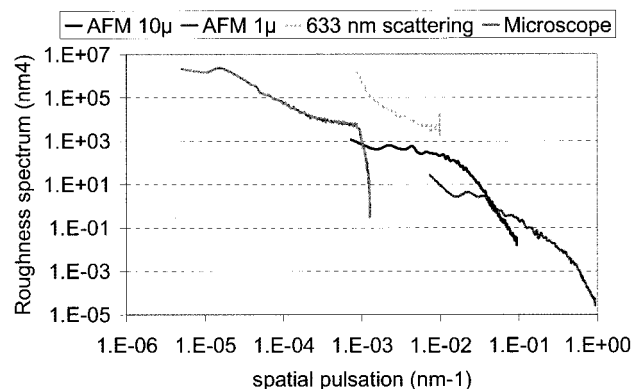


Fig. 12. Roughness spectrum deduced from AFM and 633 nm ARS measurements.

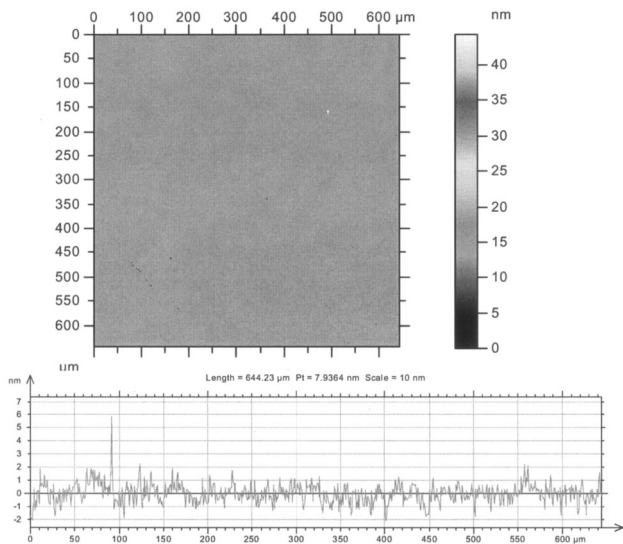


Fig. 13. OIC3 sample surface profile (coated face).

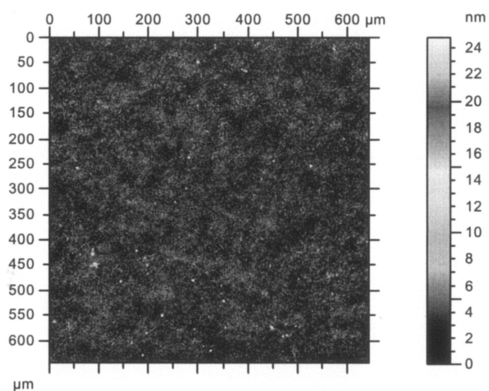


Fig. 14. OIC3 sample surface profile (rear face).

in Fig. 13 after leveling and removing of a global waviness by applying a Gaussian filter on the resulting data (square of  $0.25 \text{ mm} \times 0.25 \text{ mm}$ ). A typical line profile associated with this recording is also shown in the same figure. Around 25–50 narrow peaks of about 10–20 nm height, similar to the one observed around the 90  $\mu\text{m}$  coordinate on the previous profile, appear on the surface data. The rms

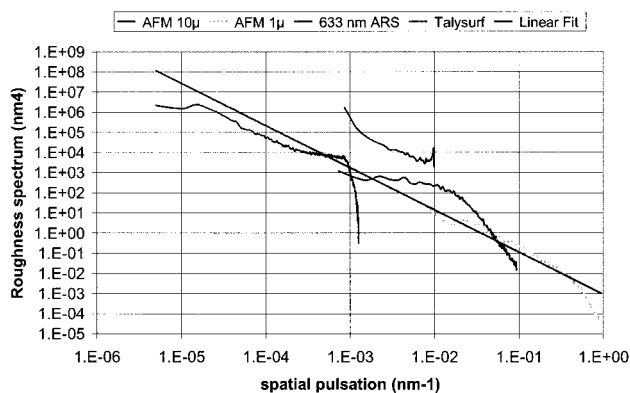


Fig. 15. Comparison of roughness spectra deduced from different methods.

roughness computed with these surface data is about 0.8 nm. Similar results are obtained on the rear face of the sample (Fig. 14, rms of about 1.2 nm).

With an approach similar to that used for AFM images, we compute the roughness spectrum for the complementary range of spatial pulsations associated with this additional characterization means (see Fig. 15). These final investigations permit us to extend the roughness spectrum spatial pulsations to a large interval, from  $10^{-5}$  to  $1 \text{ nm}^{-1}$ . The global behavior of all the spectra (AFM with two scan lengths, ARS at 633 nm, and Talysurf) is reasonably fitted in log/log units by a straight line (slope of about  $-2$ ).

#### 4. Conclusion

The optical investigation of what we learned after this study to be a  $\text{HfO}_2$  layer coated with APS technology has been performed with various experimental tools in our laboratory. Classical determination of optogeometrical parameters led to a thickness of  $189.5 \text{ nm} \pm 1 \text{ nm}$  and a refractive index of  $2.225 \pm 0.01$  (real part) and  $6 \times 10^{-3} \pm 2 \times 10^{-4}$  (imaginary part) at a wavelength of 240 nm. In addition we have measured the coating thickness spatial distribution with a standard deviation of 0.3 nm. Thanks to AFM, ARS, and Talysurf measurements, we have extended the roughness spectrum spatial pulsations to a large interval of five decades, from  $10^{-5}$  to  $1 \text{ nm}^{-1}$ . Because of the presence of pits revealed by AFM images, the rms roughness of the sample varies from 0.2 to 1 nm according to the scale and the technique of analysis.

#### References

1. J. P. Borgogno, B. Lazaridès, and P. Roche, "An improved method for the determination of the extinction coefficient of thin film materials," *Thin Solid Films* **101**, 209–220 (1983).
2. L. Abel-Tiberini, F. Lemarquis, and M. Lequime, "Dedicated spectrophotometer for localized transmittance and reflectance measurements," (in this issue).
3. C. Deumié, R. Richier, P. Dumas, and C. Amra, "Multiscale roughness in optical multilayers: atomic force microscopy and light scattering," *Appl. Opt.* **35**, 5583–5594 (1996).
4. Ph. Dumas, B. Bouffakhreddine, C. Amra, O. Vatel, E. André, R. Galindo, and F. Salvan, "Cross-characterization of surface microroughness using near field microscopies and optical techniques," *Europhys. Lett.* **22**, 717–722 (1993).
5. C. Amra, D. Torricini, and P. Roche, "Multiwavelength (0.45–10.6  $\mu\text{m}$ ) angle-resolved scatterometer or how to extend the optical window," *Appl. Opt.* **32**, 5462–5474 (1993).
6. C. Amra, "Light scattering from multilayer optics. I. Tools of investigation," *J. Opt. Soc. Am. A* **11**, 197–210 (1994).
7. C. Amra, P. Roche, and E. Pelletier, "Interface roughness cross-correlation laws deduced from scattering diagram measurements on optical multilayers: effect of the material grain size," *J. Opt. Soc. Am. B* **4**, 1087–1093 (1987).
8. D. S. Kassam, A. Duparré, K. Hehl, P. Bussemer, and J. Neubert, "Light scattering from the volume of optical thin films: theory and experiment," *Appl. Opt.* **31**, 1304–1313 (1992).
9. M. Elson, J. P. Rahn, and J. M. Bennett, "Light scattering from multilayer optics: comparison of theory and experiment," *Appl. Opt.* **19**, 669–679 (1980).
10. S. Jackobs, A. Duparre, and H. Truckenbrodt, "AFM and light scattering measurement of thin films for applications in the UV spectral region," *Int. J. Mach. Tools Manuf.* **35**, 147–153 (1997).